Carbon clusters

Chava Lifshitz

Department of Physical Chemistry and The Farkas Center for Light Induced Processes, The Hebrew University of Jerusalem, Jerusalem 91904, Israel

Abstract

Some of the most significant discoveries and achievements concerning the mass spectra and gas phase ion chemistry of carbon clusters are reviewed. These include (1) nanosecond and femtosecond laser ionizations; (2) ion structures through ion/molecule reactions, ion chromatography, and computational methods; (3) carbon cluster cooling through radiative decay, dissociative decay, and thermionic emission; (4) mechanisms and energetics of fragmentation reactions; (5) endohedral fullerenes including recent data on ion beam implantation, and (6) ion chemistry as a function of the fullerene charge state. (Int J Mass Spectrom 200 (2000) 423–442) © 2000 Elsevier Science B.V.

1. Introduction

The International Journal of Mass Spectrometry is dedicated to fundamental aspects of mass spectrometry and ion processes and to the application of mass spectrometry techniques to specific problems in chemistry and physics. It is very appropriate that an article on carbon clusters be included in the 200th volume. Ionization and mass selection have allowed the study of size-selected clusters in the gas phase. The carbon clusters in general and the fullerenes in particular owe their discovery to mass spectrometry [1,2].

This article does not attempt to give a comprehensive review on carbon clusters and not even a complete review of their mass spectrometry and gas phase ion chemistry and physics. Rather a more personal review is planned covering, out of necessity, a rather limited range of topics that have interested our laboratory in the past years. Within these topics an attempt will be made to cover the most important work done worldwide.

2. Mass spectra

Early mass spectra have shown a bimodal pattern [3,4] that has since become the well-known fingerprint of carbon clusters, namely odd and even C_n clusters for low n and only even clusters for $n \gtrsim 32$. Bimodal distributions of only singly charged ions are observed in experiments using laser vaporization of graphite or when C_{60} is ionized at low collision
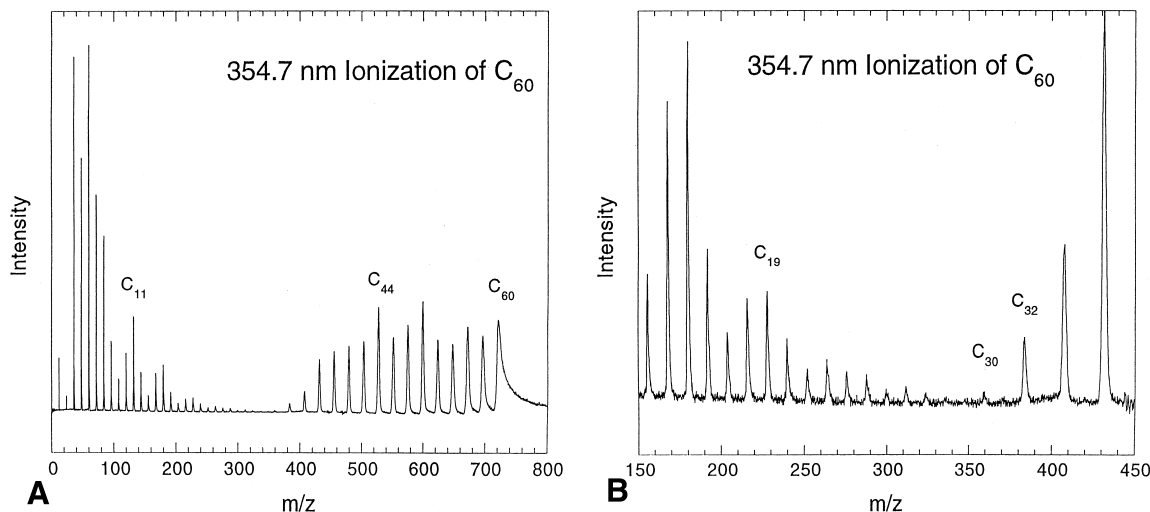
Fig. 1. (a) Time-of-flight mass spectrum using nanosecond laser photoionization of C_{60} at 354.7 nm (5 ns pulse duration) and (b) expansion of the central part of the spectrum in (a); reproduced with permission from [5].

energies or by nanosecond pulsed lasers [5], see Fig. 1. In high-energy electron impact [6] or in sub-50 fs pulsed laser ionization and fragmentation experiments [7] the mass spectra are dominated by multiply charged ions and their fragments, see Fig. 2. At low collision energies or long time scales the excitation is predominantly via vibrational degrees of freedom. In experiments leading to multiply charged ions the initial excitation is electronic and occurs on a time scale that is fast compared to the electron–phonon coupling time [7].
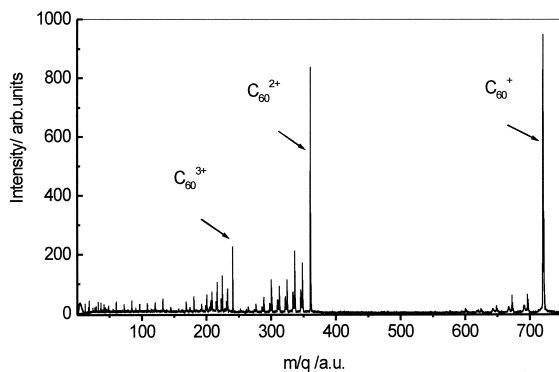
The even carbon clusters with $n \gtrsim 32$ are now known to be fullerenes, all of them undergoing consecutive evaporations of C_2 units [8]. Giant fullerenes at least as large as C_{600}^+ have been observed. The ions with $n = 60$ and $n = 70$ are particularly abundant ("magic numbers") and of special stability and their neutral counterparts have of course been synthesized in macroscopic quantities [9] since their early mass spectrometric discovery [1]. Among the low-mass ions with odd numbers of carbon atoms those with $n = 7, 11, 15, 19,$ and 23 are particularly abundant (magic) [3–5,8,10].

3. Ion structures; ion chromatography

The synthesis of C_{60} and C_{70} [9] has opened the way for a multitude of techniques for structure determination including nuclear magnetic resonance (NMR), x-ray diffraction and IR spectroscopy and the fullerene structures of these two species are well established. Smaller carbon clusters have not been isolated and the structures of the corresponding ionic clusters have been indirectly determined. The spectroscopy, structure, and energetics of small carbon clusters have been reviewed recently [11,12]. Density
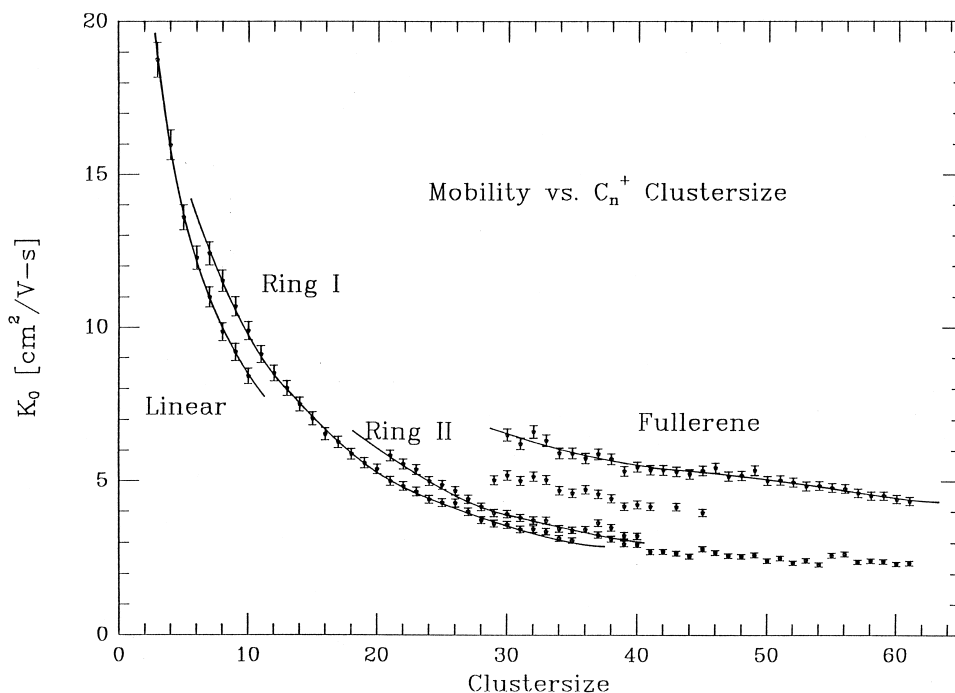

Fig. 2. Time-of-flight mass spectrum using femtosecond laser photoionization of C_{60} at 795 nm (35 fs pulse duration); reproduced with permission from [7].

Fig. 3. Plot of the mobility vs. cluster size for the positively charged carbon cluster ions C_n^+ from $n=3$ to $n=60$; reproduced with permission from [16].

functional theory (DFT) and coupled-cluster ab initio calculations [13,14] have been crucial and were carried out in concert with experiments.

Of special significance has been the first evidence, obtained through ion/molecule reactions with D_2, of structural isomers for the C_7^+ cluster system [10]. Ion/molecule reactivity patterns suggested the existence of a linear and a cyclic form of the C_7^+ ion and a structural change from linear to monocyclic rings in the cluster ions between $n = 9$ and 10 [15]. A real breakthrough in the structure determination of gas phase ions in general and carbon clusters in particular came with the development of the technique of ion chromatography [16–22]. The ion chromatography device combines mass selection with ion mobility measurements in a drift cell filled with helium. It separates ions that have the same mass but differ in isomeric structure according to their arrival time distributions at the detector. Pioneering results obtained by Bowers and co-workers [16], for ion mobility versus C_n^+ cluster size, are presented in Fig. 3.

Ion chromatography has demonstrated unequivocally that carbon clusters grow first in chains, transform to monocyclic planar rings at about C_{10} and form new families of planar bi-, tri-, and tetracyclic rings at C_{20}, C_{30}, and C_{40}, respectively. Fullerenes appear at C_{30} and dominate by C_{50}. The isomeric distribution patterns of positively charged and negatively charged clusters are similar but not identical with the anions demonstrating a relatively low abundance of fullerenes [22]. The structural data when coupled with annealing studies [19,23–27] indicate that fullerenes are formed from isomerization of hot planar ring systems. The monocyclic ring is a relatively stable isomer for many of the carbon cluster ions including C_{60}^+ [27] and is the only stable isomer for C_n^+ ($n = 11$–20) [22]. The cyclic isomer is the most stable form for C_7^+ [18] in agreement with results deduced by ion/molecule reactions [10,15].

The special stability of C_{60} is due to its geometrical structure—the truncated icosahedron with isolated pentagons—and is reflected in all of its ions. The

"magic" nature, i.e. special stability of ions C_n^+ ($n = 7, 11, 15, 19,$ and 23) referred to earlier, is due to their planar and cyclic characters and to the presence of ($4k + 2$) π electrons ($k = 1–5$ and $n = 4k + 3$); they fulfill the Hückel rule of aromaticity. This stability of the monocyclic aromatic ions is due to their electronic properties and does not reflect a special stability of the corresponding neutrals. The neutrals predicted to be aromatic are rather C_6, C_{10}, C_{14}, C_{18}, and C_{22}, respectively. The existence of cyclic C_6 has been predicted theoretically [14] and observed experimentally [28]. It has long ago been predicted [29] that C_n rings with $n = 4k + 2$ become more stable than the corresponding linear chains for $n \gtrsim 10$. Ultraviolet photoelectron spectra of the corresponding negative ions have verified this in 1988 [30]. It has furthermore been demonstrated for C_{10} that the cumulenic delocalized ring structure that is aromatic is more stable than the one with alternating single–triple bonds [31]. This delocalized structure has ten pi bonds, five are perpendicular to the ring and five are in the plane of the ring. The former constitute a regular aromatic system, the latter an in-plane aromatic system. As a result, C_{10} (and presumably also C_{11}^+) may be considered having "double" or "super" aromaticity. A very nice example of the stability due to aromaticity has been observed in the fragmentation pattern of C_{37}^+ injected at a high energy into an ion chromatography experiment [19(c)]. The products are C_{15}^+, C_{19}^+, and C_{23}^+ formed together with C_{22}, C_{18}, and C_{14}, respectively, indicating the double stability of the ring products—ionic as well as neutral.

The cyclic ion C_{13}^+ has $4k$ π electrons ($k = 3$ and $n = 4k + 1 = 13$) and is therefore antiaromatic. As a result it is very unstable [32] and demonstrates high reactivity in its ion/molecule reactions with various neutrals [33–35]. The reactivity pattern demonstrates the expected fourfold periodicity with C_{17}^+ being quite reactive as well [33–37].

Carbon cluster ions may be generated by electron impact induced fragmentation of perchlorinated polycyclic aromatic compounds (PPA) [32–35,38,39]. The properties of the two groups of C_n^+ clusters—those made by laser vaporization of graphite and the ones made by dissociative electron ionization—were found to be remarkably similar, suggesting similar structures, irrespective of the mode of production [32]. Hoffman [29] has already predicted that polycyclic fragments of a graphite lattice are very unstable relative to simple polygons with the same number of atoms. Ion chromatography was able eventually to demonstrate unequivocally [40] that polychlorinated graphitic (PPA) precursors of carbon ion clusters, when stripped of all of their chlorine atoms, form monocyclic rings, certainly in the case of C_{12}^+. The ions C_{20}^+ and C_{24}^+ formed by laser desorption of graphite were demonstrated to be cyclic [41]. To the best of our knowledge, the search for C_{20}^+ and C_{24}^+ graphitic ions using PPAs was unsuccessful. Calculations predict such structures with C_{20} being a corannulenelike bowl [42] and C_{24} having either a coronenelike planar sheet or a fullerene as the most stable structure [43].

4. Cluster cooling

Hot carbon clusters can cool down by several parallel processes including emission of photons (radiative decay), evaporation of neutral fragments (dissociative decay) and electron emission (delayed ionization or "thermionic emission." The understanding of the intricate interplay between these various cooling processes although being of great current interest is still in its infancy. These processes have been studied in some detail both experimentally and theoretically particularly for C_{60} but also for other carbon clusters. The topic of "delayed ionization and fragmentation en route to thermionic emission" has been reviewed thoroughly recently [44].

4.1. Radiative decay

The optical emission spectra of laser desorbed C_{60} have been determined by Mitzner and Campbell in a pioneering study [45]. The spectra that were observed were structureless, demonstrating close similarities to blackbodylike radiation, and could be fitted with the Planck blackbody formula. The derived temperatures were of great interest since pulsed laser desorption of
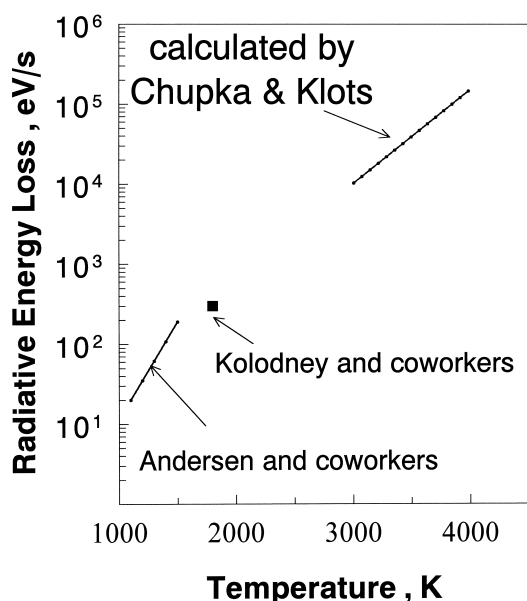
Fig. 4. C_{60} radiative decay rates as a function of temperature; adapted by [166] from various sources as indicated: Kolodney and co-workers ([46]); Andersen and co-workers ([47]; Chupka and Klots ([51]).

fullerenes has been used extensively as an ion source for time-of-flight (TOF) mass spectrometry and to produce beams of charged fullerenes in collision experiments [45]. It was concluded that blackbody radiation is the dominant cooling mechanism below about 3000 K. At higher temperatures the molecules will rapidly cool by emitting an electron and/or a C_2 fragment.

Radiative cooling rates have been determined experimentally through their competition with C_2 evaporation or electron emission. Some experimental results are summarized in Fig. 4. An estimate of the cooling rate at $T \simeq 1800$ K was obtained by Kolodney and co-workers [46] from observation of the depletion of thermal C_{60} beams by fragmentation. The dissociation kinetics of neutral C_{60} was used as a thermometric probe and the result is included in Fig. 4. Radiative cooling of C_{60}^- can be followed by thermionic emission as a function of time after injection into a heavy-ion storage ring. In this experiment the electron emission is used as a calibrated thermometer to measure the cooling rate [47]. The advantage of

this method is that the electron affinity of C_{60} is very accurately known [48,49] and the radiative rate can be determined over a range of temperatures (included in Fig. 4). The radiative cooling rate of C_{60}^+ can be determined through its competition with C_2 evaporation [50]. The method employs two-electron dissociative ionization of C_{60} at electron energies where the single electron dissociative ionization process does not occur. In the internal energy range (19 ± 3.5) eV (~ 1800 K) the mean radiative rate is $k_{rad} = (3.3 \pm 1) \times 10^2$ s^{-1} [50]. Since the photon energy emitted is of the order of 1 eV this result is in quite good agreement with that of Kolodney et al. [46]. Experimental results are lacking at higher temperatures at which competition with C_2 evaporation from C_{60}^+ takes place. Computations were carried out in this energy range by Chupka and Klots [51], albeit for neutral C_{60} [51]. Two models were employed: (1) calculations based on measured oscillator strengths and (2) a modified blackbody model. Whether a blackbody model is applicable for the emission of radiation from C_{60} or its ions is controversial [51]. The authors concluded that the oscillator treatment is superior to the blackbody model and their results are included in Fig. 4. The conversion between the internal energy, E, and the temperature, T, necessary to deduce the data of Fig. 4 from the computations is based on the isokinetic relationship of finite heat bath theory (FHBT) [51,52].

The radiative decay rates deduced between ~ 3000 and 4000 K (in the range of energies $E \simeq 40$–50 eV) are much higher than originally anticipated [53] since emission is in the visible due to electronic transitions and not in the infrared due to vibrational transitions. This causes the very large kinetic shift observed for the appearance energy of C_{58}^+ from C_{60} [54–56]. Radiative cooling has been demonstrated to suppress the fraction of metastable fullerene ions undergoing C_2 evaporation in the field free region of a TOF mass spectrometer (the so-called "metastable fraction") [57]. Time resolved metastable fractions (MFs) for C_2 evaporations from C_n^+ ions measured on an ion trap/reflectron mass spectrometer were modeled using microcanonical dissociative as well as radiative decay rate constants [58,59]. Dissociative decay is important for C_{60}^+ at short times but radiative decay is already a
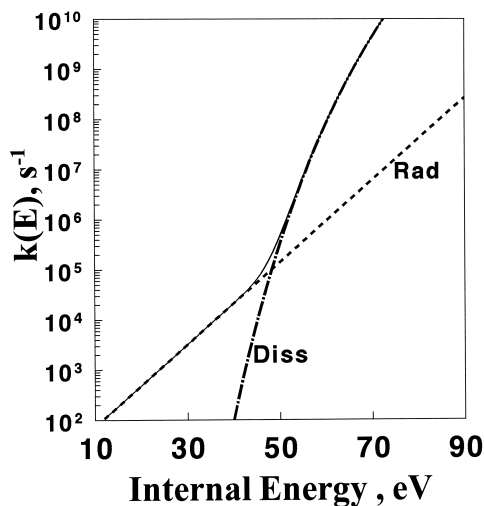
Fig. 5. Microcanonical rate constant, $k(E)$ in seconds^{-1}, as a function of energy, E in electron volts, for dissociative decay (dot-dashed line) and radiative decay (short dashed line) of C_{60}^+. Dissociation involves elimination of C_2; radiative decay is in the visible and has been modeled following [51,59]; reproduced with permission from [60].

strongly contributing factor on the microsecond time scale and becomes the dominant channel at 30 μs as judged from theoretical modeling of time resolved kinetic energy releases [60]. As a result, in two-sector field instruments fullerene ions will decay predominantly via dissociation at the entrance to the first field free region and predominantly by radiative decay at the exit from the second field free region. This is a direct outcome from the crossing between the corresponding rate energy, $k(E)$, dependences (Fig. 5).

4.2. Delayed ionization; thermionic emission

One of the fascinating properties of carbon clusters is the phenomenon of delayed ionization termed thermionic emission, a property known for bulk matter. The phenomenon has been first observed for positive singly charged giant fullerenes in the size range from 100 to 600 atoms, whose second ionization energies are relatively low [61]. Intense laser excitation of the magnetically levitated trapped fullerene ions at 4.0 eV was found to result in production of multiply charged ions. Details of the

time scale of this process suggested it was due to thermionic emission from the superheated gas phase clusters. Clear-cut delayed ionization with average lifetimes on the order of several μsec was first observed for C_{60} and C_{70} by Campbell and co-workers [62] followed by Wurz and Lykke [63]. This showed up in the by now well-known long "tails" to the high mass sides of the C_{60}^+ and C_{70}^+ peaks in TOF mass spectra (see also Fig. 1). This delayed ionization has been termed thermionic emission signifying the coupling of rovibronic and electronic states in the molecule [62]. No tailing on the peaks is observed upon ionization by femtosecond lasers [64]. Direct ionization of C_{60} by multiphoton absorption is in competition with delayed ionization and fragmentation [65]. This phenomenon has been studied recently [64] in greater detail by measuring the laser pulse duration dependence of C_{60} photoelectron spectra. Direct multiphoton ionization was observed for short 25 fs pulses whereas delayed ionization sets in for pulse durations on the order of a picosecond that are long enough to allow coupling to the vibrational degrees of freedom. High internal energies ($\approx$50 eV) are achieved by absorption of 10–20 photons in the visible or in the UV and conversion from electronic to vibrational excitation [65]. Infrared multiphoton excitation, dissociation and ionization of C_{60} have also been observed [66]. Thermionic emission is also well known for negative fullerenes, particularly C_{60}^- [47,67,68], see Fig. 6. Thermal emission of electrons from C_{60}^- is enhanced after absorption of photons. This process has been utilized to measure the photoabsorption cross sections of hot C_{60} anions in the visible and near-infrared [68].

Several questions have been raised recently [69] concerning the statistical nature of delayed ionization, i.e. its "thermionic" character. The possibility has been raised that the internal energy is not equipartitioned amongst all the modes, and only a subset of the electronic states are coupled to the vibrations. Singlet–triplet intersystem crossing in C_{60} and intramolecular interaction of many triplet states have already been pointed out earlier to be important for thermionic emission [70].

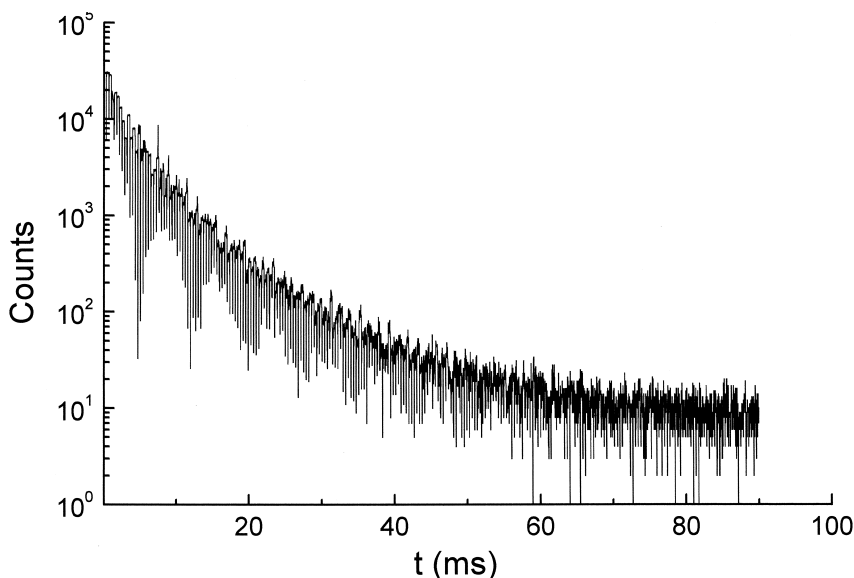Quasiequilibrium rate constant calculations for

Fig. 6. Rate of decay by thermionic emission of a stored C_{60}^- beam. Negative fullerene ions are produced in a plasma ion source and injected into the ion storage ring ASTRID. The signal measured is the number of neutral molecules hitting the detector at one corner of ASTRID. During the 100 ms storage period, the anions emit electrons spontaneously, with a rapidly decreasing rate; reproduced by permission from ref. [68].

thermionic emission [71] implicitly assume statistical behavior. If the newly activated molecule is in a state that does not interconvert rapidly with the full phase space available, rate constants will be unpredictable [72]. Most calculations have assumed complete energy randomization but other models are also being developed [44]. Early calculations of the thermionic emission rates as a function of internal energy or as a function of temperature yielded results that were nearly parallel or even overlapping with the corresponding dissociative rates for C_{60} [45,65,66,72,73]. However in more recent calculations [74] the rate energy curves, $k(E)$, for dissociation (C_2 evaporation) and thermionic emission of neutral C_{60} cross one another (Fig. 7) and diverge at high energies. According to the recent model, dissociation is dominant at high energies, although it has a high activation energy, since it has a very loose transition state. The activation parameters used for
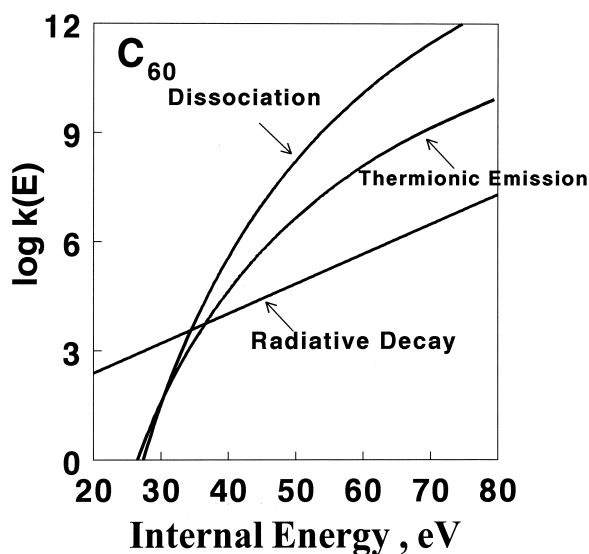
$$C_{60} \rightarrow C_{58} + C_2 \tag{1a}$$

$$C_{60} \rightarrow C_{60}^+ + e^- \tag{2}$$

Fig. 7. Microcanonical rate constant, $k(E)$ in seconds^{-1}, as a function of energy, E in electron volts, for dissociative decay, thermionic emission and radiative decay of neutral C_{60}, reactions (1a), (2), and (3a), respectively. The activation parameters for reactions (1a) and (2) are given in the text. The radiative decay rate can be cast in the form: $\log k(E) = 0.082E + 0.744$; reproduced by permission from [74].

in Fig. 7 are: Arrhenius pre-exponential A factors, $A(1a) = 8 \times 10^{20}$ s^{-1}; $A(2) = 2 \times 10^{16}$ s^{-1}; activation energy for reaction (1a) (=vaporization energy) $\Delta E_{vap}(1a) = 10$ eV; activation energy for reaction (2) (=ionization energy) IE(C$_{60}$)=7.6 eV.

Reactions (1a) and (2), dissociative decay and thermionic emission, respectively, and

$$C_{60}^* \rightarrow C_{60} + h\nu \qquad (3a)$$

radiative decay, are important for neutral C$_{60}$. However, thermionic emission has been neglected in the case of C$_{60}^+$ (Fig. 5) since the second ionization energy—the ionization energy of C$_{60}^+$—is very high, IE(C$_{60}^+$) = 11.36 $\pm$ 0.05 eV [75,76]. Further, due to the high C$_2$ binding energy (10 eV or higher [74]) dissociative decay can be neglected in the case of C$_{60}^-$—only thermionic emission and radiative decay need to be considered as competitive processes in a statistically behaving C$_{60}^-$ system [47]. It has been demonstrated [77] that higher fullerenes, C$_n$ for at least up to $n = 96$, can be efficiently transformed into delayed positive ions but aggregates of fullerenes (C$_n$)$_m$ do not undergo thermionic emission because they fragment rapidly without ever reaching the temperature of 3000–4000 K required for delayed ionization. As a result, delayed ionization may be utilized to distinguish between higher fullerenes and other, more loosely bound, carbon aggregates [77].

Whether dissociation is the dominant decay process of C$_{60}$ at high energies remains an open question. The efficiency of thermionic emission has been determined [78] over the time interval 0.1–80 μs to have a lower limit of 2.6 $\pm$ 1.1%. The rate of thermionic emission has a power-law dependence. The value of the exponent provides information about the competition between dissociation and thermionic emission and is equal to the ratio of the ionization energy that is accurately known and the activation energy for fragmentation. This has led to a determination of the C$_2$ binding energy that is independent of assumptions concerning the looseness of the transition state [79].

5. Mechanisms and energetics of fragmentation reactions

5.1. Short background

Unimolecular, collision induced and surface induced decompositions of selected carbon cluster ions were reviewed by us some years ago [80].

Bowers and co-workers studied [81–85] in pioneering work the unimolecular reactions, metastable fractions and kinetic energy releases (KERs) in carbon ion clusters. They used tandem mass spectrometry techniques on ions generated by laser vaporization of graphite. The first electron ionization mass spectrometry study of synthetic C$_{60}$ [86] has included high energy collision activated dissociation (CAD) of C$_{60}^+$ and C$_{60}^{2+}$. It demonstrated the successive loss of C$_2$ units. Under high-energy multiple-collision conditions [87] and in laser photodissociation experiments [88] the end point for C$_2$ loss from C$_{60}^+$ is C$_{32}^+$.

5.2. Elimination of C_{2n} or n consecutive C_2 eliminations

One interesting question addressed since our early review [80] has been whether there is emission of C$_4$ or sequential emission of C$_2$ upon unimolecular decay of singly and multiply charged fullerenes [89] and whether large neutral moieties are liberated upon CAD of C$_{60}^{z+}$ [90]. Tandem mass spectrometry has provided direct experimental evidence [89] that C$_{60}^{z+}$ ($z = 1$, 2, or 3) and C$_{58}^{z+}$ ($z = 1$ or 2) undergo unimolecular dissociation by sequential emission of two C$_2$ units, on a time scale of 10^{-5} s. This was done by selecting product ions from C$_2$ loss in the first field-free region of a reverse geometry magnetic sector instrument and using the electric sector to identify further loss of C$_2$ from fragment ions in the second field-free region. It was concluded furthermore that C$_4$ elimination is an unimportant unimolecular reaction channel [89]. On the other hand neutral fragment reionization [90] has demonstrated unequivocally that CAD of C$_{60}^{z+}$ ($z = 1$–4) liberates large C$_{2n}$ fragments (up to C$_{28}$ for $z = 1$). These are high-energy processes that do not compete with the

unimolecular elimination of C_2 on the microsecond time scale.

5.3. Electron ionization and breakdown curves

Electron ionization has been crucial in providing us with breakdown curves for the consecutive eliminations of C_2 from C_{60}^+ in pioneering work of Märk and co-workers [91]. No other experimental source is currently available for this very basic attribute of fullerene mass spectra. Attempts at coincidence measurements using synchrotron radiation failed since no threshold electrons were detected upon photoionization of C_{60} [92]. Experimental breakdown curves were obtained by taking second derivatives of the electron ionization efficiency curves of the fragment ions [91,93]. The statistical nature of the unimolecular fragmentation of C_{60}^+ became immediately apparent. There is a large kinetic shift for the formation of C_{58}^+ however consecutive fragmentations already benefit from the high internal energy content with which C_{58}^+ is formed and there is a relatively small, nearly constant, energy increment ($\sim$5–6 eV) required for them. The breakdown curves were calculated theoretically [91,93] using FHBT and Rice-Ramsperger-Kassel-Marcus (RRKM) theory. These models were used to deduce the C_2 binding energy in C_{60}^+ and a self-consistent set of binding energies for the lower fullerenes using experimental appearance energies.

5.3. C_2 binding energy and C_{60} dissociation mechanism

The original model calculations of the electron ionization breakdown curves assumed a fairly tight transition state for

$$C_{60}^+ \rightarrow C_{58}^+ + C_2 \tag{1b}$$

and led to an upper limit for the binding energy C_{58}^+–C_2 of approximately 7.6 eV. The calculations were redone recently [59] leading to a re-evaluation of the C_2 binding energy in favor of a value in excess of 9.5 eV. The recent calculations used a very loose

transition state for reaction (1b) with an activation entropy, $\Delta S^{\#} = 18.8$ eu and included radiative decay,

$$C_{60}^{*\,+} \rightarrow C_{60}^+ + h\nu \tag{3b}$$

in the modeling.

The current status of the C_2 binding energy in C_{60} (ionic and neutral) has been reviewed by us recently [74]. All of the recent experiments favor a high C_2 binding energy, in excess of 10 eV in the neutral and in excess of 9.5 eV in the cation, in agreement with DFT and second order Møller-Plesset calculations [94]. The experiments include kinetic energy release distributions (KERDs) [95–97], time-resolved KERs [60], time-resolved metastable fractions [59], and thermionic emission [79]. In spite of this agreement between experiment and theory there is still an ongoing controversy concerning this binding energy (see Fig. 1 of [74]).

The dissociation mechanism of C_{60} has been studied through ab initio calculations [98–100]. C_2 elimination is a multiple step process. The last step involves formation of a C_{58} isomer containing a seven-membered ring to which a C_2 "stick" is loosely bound. The C_2 molecule that leaves the surface is due to a bond shared by a hexagon and a pentagon (5–6 bond).

5.4. Magic shells

The dissociation energies of small carbon cluster ions (C_{2-19}^+) were determined from collision induced dissociation thresholds [101,102]. Clusters in the range C_{10-19}^+ demonstrate the expected fourfold periodicity. Relative dissociation energies of the fullerenes were determined from metastable fractions [57,59,74,103–105], electron ionization appearance energies [6,91,93,106], theoretical calculations [107], and endothermic charge transfer [108]. Whether $n = 60$ is a magic number for C_n^+ clusters or part of a "magic shell" [103,104] remains an open question. There is general agreement that C_{58}^+ is less stable than C_{60}^+ and that C_{62}^+ is considerably less stable. However, some results demonstrate a dramatic drop in dissociation energy in going from $n \lesssim 60$ to $n > 60$
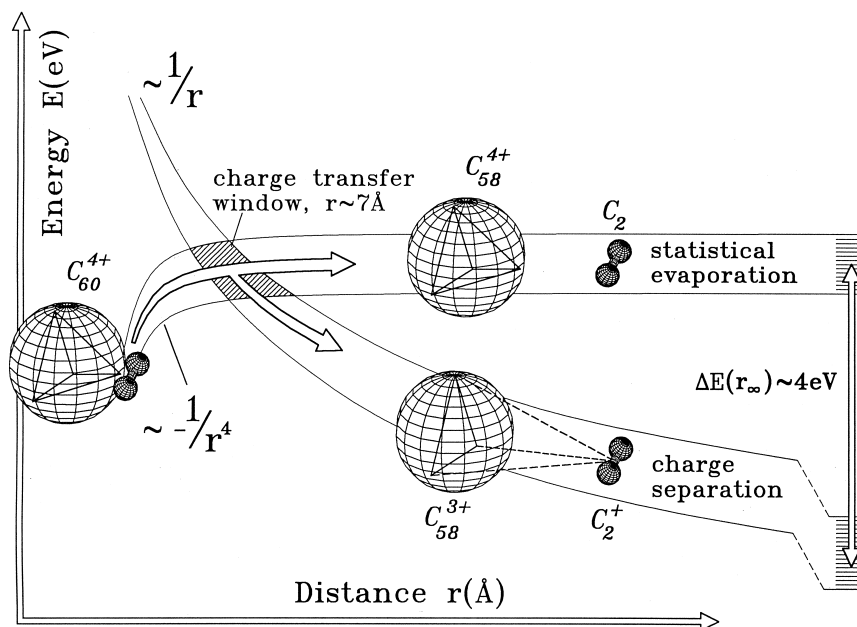
Fig. 8. Schematic representation of the spontaneous decay of C_{60}^{4+} using the curve crossing model; reproduced by permission from [110].

interpreted in terms of magic shells [103] whereas other results find the relative dissociation energies for large fullerenes, with $n > 60$, to be at about the same level as those for $n < 60$ [105].

5.5. Fission reactions

Multiply charged positive fullerene ions undergo superasymmetric fission reactions [109–112],

$$C_{60-2m}^{z+} \rightarrow C_{60-2m-2}^{(z-1)+} + C_2^+ \qquad (4)$$

With m ranging from 0 to 7 and z from 3 to 7. These reactions were demonstrated to take place in three stages. They are initiated by neutral C_2 evaporation followed by an electron (charge) transfer process from the receding neutral fragment to the remaining highly charged fullerene ion cage leading finally to coulomb repulsion between the two charged reaction products. The mechanism is similar to the avoided crossing model of Gill and Radom [113]. It is shown schematically in Fig. 8. The intercharge distance at the point of charge transfer was calculated from the KER to be about 7 Å [110].

5.6. Fragmentation by surface impact

Scattering experiments of C_{60}^+ and C_{60}^- ions from surfaces were among the first to demonstrate the exceptional stability of fullerenes [114] and to propose the very high C_{58}–C_2 binding energy in excess of 10 eV [115]. Thermionic emission discussed above is also an important result of surface impact [115–117]. Neutralization and delayed ionization in fullerene surface collisions have been studied with the aim of deducing activation energies from fragmentation and ionization rates [118]. Since a tight transition state was assumed in the RRKM calculation the result deduced for the C_{58}^+–C_2 binding energy from the surface collision experiments was 6.6 ± 0.5 eV in agreement with experimental values acceptable at the time the data were obtained. The surface-induced-dissociation (SID) of C_{60}^+ and higher fullerenes on impact with highly oriented pyrolitic graphite (HOPG) was observed to lead to consecutive C_2 elimination in the energy range 150–650 eV [119]. At higher impact energies fragmentation leads to "shattering." Smaller even and odd numbered C_n^+ clusters
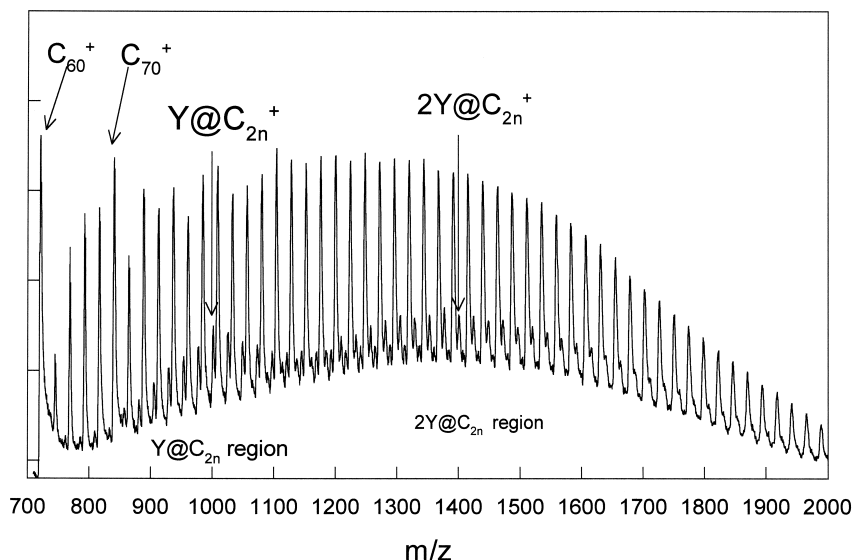
Fig. 9. Time-of-flight mass spectrum of an yttrium containing fullerene sample prepared by the arc discharge technique. The sample is desorbed by a 1064 nm Nd-YAG laser and ionized with a second laser at 352 nm. Note that the lower fullerenes are singly occupied whereas the higher ones are mostly doubly occupied. Results given in [167].

appear having the well-known characteristic distribution (see Fig. 1) observed also for nanosecond multiphoton fragmentation [120] and high-energy gas phase collisions [121,122]. Since the pattern observed was independent of the excitation method it was concluded [119] that the fragmentation mechanism is statistical and characterized by rapid energy conversion into vibrational degrees of freedom.

One of the controversial aspects of SID experiments with fullerene ions has been the conversion efficiency of translational into internal energy that may be surface dependent. A recently determined value for C_n^+ ions in the range $50 \lesssim n \lesssim 60$ colliding with a hydrocarbon-covered stainless steel surface is $6.8 \pm 0.5\%$ [123]. A similar conversion efficiency adopted previously by Beck et al. [119] led to the conclusion that the transition from sequential C_2 fragmentation of C_{60}^+ to the high energy shattering takes place at around 70 eV internal energy. At an energy of 70–80 eV a so-called phase transition occurs according to molecular dynamics simulations and according to a simple statistical model [124,125], in which the fullerene cage is transformed to a disordered assembly of carbon rings and chains [119].

The elimination of large neutral C_{2n} fragments under high energy CID [90] alluded to earlier is most probably related to this "catastrophic" event.

6. Endohedral fullerenes

6.1. Short background

One of the fascinating properties of fullerenes is their ability to trap atoms and small molecules inside the cage. The first evidence for endohedral metallofullerenes was reported soon after the discovery of C_{60} in 1985 [126]. However, only in 1991 could endohedral metallofullerenes be isolated in macroscopic amounts. This was achieved by using laser- or arc-vaporization [127] of graphite-metal composites in helium. We have recently prepared by arc-vaporization an yttrium sample whose mass spectrum is presented in Fig. 9.

Schwarz and co-workers in high-energy ion beam collision experiments [128,129] have first observed endohedral fullerenes with a noble gas atom inside the fullerene cage. Saunders and co-workers have shown
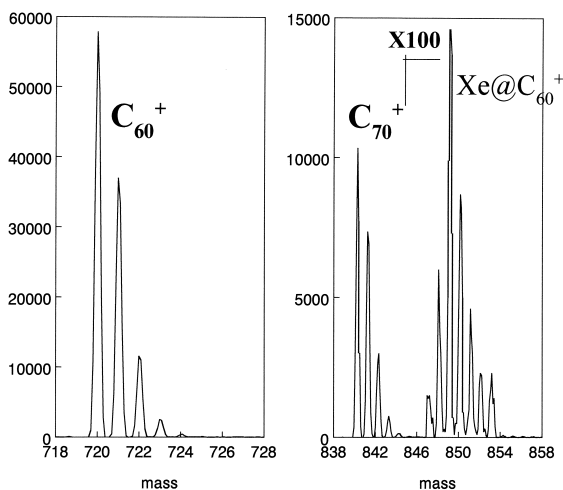
Fig. 10. Mass spectrum of an endohedral $Xe@C_{60}$ containing fullerene sample. The xenon was 75% enriched ^{129}Xe. The sample was prepared by the high-pressure high-temperature incorporation technique [130,131]. The mass spectrum was obtained by electron impact ionization on a ZAB-2F reverse geometry magnetic sector instrument. A 0.25% degree of incorporation of ^{129}Xe is observed. Unpublished results given in [168].

that neutral noble gas compounds can be prepared by heating fullerenes under high pressure of a noble gas [130,131]. Endohedral fullerenes of all the noble gases were prepared using this method. Typical yields of incorporation are around 0.2% for helium, neon, argon and krypton and around 0.04% for xenon. Recent experiments have been more successful and a spectrum of the xenon compound we have obtained (Fig. 10) shows a considerably higher degree of incorporation.

A recent exciting finding, using laser desorption and noble gas mass spectrometry on the fullerenes from the Allende and Murchison meteorites, has been that fullerenes are an extraterrestrial carbon carrier phase for noble gases [132]. The fullerenes in these meteorites were demonstrated to contain endohedral helium. A very high $^{3}He/^{4}He$ ratio was observed for them, ~150 times greater than the ratio in the earth's atmosphere, and similar to the value estimated for the early solar system.

6.2. Rice "shrink wrap" mechanism [8]

Most ionic endohedral species studied, including lanthanide containing and noble gas atom containing

ones are known to withstand the shrink-wrap test until they reach a critical radius [133]. In other words, they do not lose the endohedral atom but rather evaporate C_2 units consecutively leading in each step to the lower fullerene. For example, $He@C_{60}^+$ does not undergo

$$He@C_{60}^+ \xrightarrow{\;\;x\;\;} C_{60}^+ + He \qquad (5)$$

loss of a helium atom but rather C_2 elimination,

$$He@C_{60}^+ \rightarrow He@C_{58}^+ + C_2 \qquad (6)$$

even under high-energy collision experiments [128]. If endohedral fullerenes are assumed to behave statistically, this observation might indicate a lower activation energy for reaction (6) and/or a higher activation entropy. Perhaps in spite of favorable energetics, reaction (5) does not take place and the unimolecular reaction system is not statistical (i.e. one is dealing with "non-RRKM-like behavior"). The energetics of these reactions is still controversial.

The effect of a series of endohedral atoms on the fullerene C_2 binding energy has been studied indirectly [134,135] through the measurements of KERs. Kinetic energy release distributions were measured for the emission of C_2 units from the positive ions of C_{60}, $Ne@C_{60}$, $Ar@C_{60}$, $Kr@C_{60}$, C_{82}, $La@C_{82}$, $Tb@C_{82}$, C_{84}, and $Sc_2@C_{84}$. These distributions were analyzed using both a model free approach [103,136], and a formalism developed by Klots, based on decomposition in a spherically symmetric potential [72,137]. The C_2 binding energies were deduced from the models. Noble gas atoms were shown to stabilize the fullerene cage. The C_2 binding energies increase in the order: $\Delta E_{vap}(C_{60}^+) < \Delta E_{vap}(Ne@C_{60}^+) < \Delta E_{vap}(Ar@C_{60}^+) < \Delta E_{vap}(Kr@C_{60}^+)$. Endohedral metal atoms have a strong effect on the cage binding. The C_2 binding energy in $La@C_{82}^+$ is about 2 eV higher than that in C_{82}^+ (note added in proof [135]). The Tb atom has an even stronger effect with a binding energy of about 4 eV higher than for C_{82}^+. The emission of a C_2 unit from the dimetallofullerenes $Sc_2@C_{84}^+$ and $Tb_2@C_{84}^+$ was studied as well. Two Sc atoms have

a slight destabilizing effect on C_{84}, whereas two Tb atoms stabilize the cage.

6.3. Artificial noble gas molecules inside fullerenes

Mass spectrometry was instrumental in demonstrating the existence of endohedral noble gas fullerenes. We have recently demonstrated using mass spectrometric techniques, the existence of artificial noble gas molecules inside neutral fullerenes, first for Ne_2 [138] and later for He_2 [139]. The species are ionized by electron impact. A wide dynamic range is required in order to observe them mass spectrometrically. The He_2 "molecule" can also be observed by ^3He NMR [139]. High-temperature and high-pressure labeling of C_{70} with ^{22}Ne or ^3He led to a ratio of empty C_{70} to mono-occupied to di-occupied of 1000: 1:0.02, for Ne and 37:1:0.05, for He, respectively. If the incorporation of each atom into the fullerene molecule were an independent event, one would predict a much lower degree of di-occupation. A mechanism where a small fraction of the fullerene breaks open and reaches equilibrium with the noble gas and then closes was suggested to explain the result [138]. A so-called promoter (free radical?) is responsible for the window-opening process in the fullerene, a model that has also gained some theoretical support [140].

Putting a pair of noble gas atoms inside a fullerene cage effectively creates an artificial molecule. The atoms are forced into contact by the cage and vibrate and rotate within the cage in the same manner as a diatomic molecule. Schwarz and co-worker [141] had observed earlier in pioneering work the sequential insertion of ^3He and ^4He into C_{60}^+. However these doubly occupied species were observed at the time only on the short time scale (microseconds) of an ion beam/collision chamber experiment. The neutral species observed more recently [138,139] have long shelf lives. If they will eventually be produced in larger quantities then this will allow other spectroscopic techniques besides mass spectrometry and NMR to be applied.
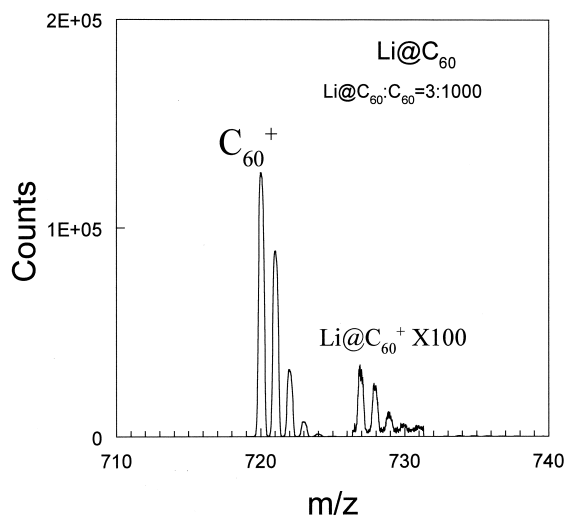

Fig. 11. Mass spectrum of an endohedral $^7Li@C_{60}$ containing sample. The sample was prepared by ion implantation [142]. The mass spectrum was obtained by electron impact ionization on a ZAB-2F reverse geometry magnetic sector instrument. Results given in [169].

6.4. Ion implantation; Li@C$_{60}$; N@C$_{60}$ and N@C$_{70}$

Endohedral metallofullerenes are prepared by the arc discharge method by adding the appropriate materials during the formation of the fullerenes. High temperatures and high pressures are employed for the encapsulation of noble gas atoms into C_{60}. Endohedral compounds can also be prepared by ion implantation. This technique has been applied to lithium and other alkali atom fullerenes [142], to noble gas fullerenes [143] and to noble gas containing dodeca-hedrane [144]. We have ionized a mixture of the lithium compound $^7Li@C_{60}$ in C_{60} by electron impact and a characteristic mass spectrum with its ^{13}C isotope pattern is clearly observed (Fig. 11).

A particularly interesting endohedral compound that has been produced by the ion implantation technique is N@C$_{60}$ [145]. The most distinct feature of N@C$_{60}$ is that an extremely reactive atom (atomic nitrogen) is stabilized in its electronic ground-state configuration by the protective shielding of C_{60} [146]. The fullerenes are protective cages, for the atomic nitrogen, that have been termed "chemical Faraday cages" [147]. Since the encapsulated atom keeps its

atomic structure, the electron paramagnetic resonance (EPR) technique was found to be extremely useful in the investigation of this system [147–149]. We have recently studied N @ C_{60} and N @ C_{70} mass spectrometrically [150]. We are certain that we have ionized the endohedral compounds in these experiments because we obtained their characteristic EPR spectra. Prior to this there has been no serious mass spectrometric study of these compounds. The earliest experiments yielded a concentration of only 10^{-7} paramagnetic centers per C_{60} molecule and mass spectrometric identification of the complex was difficult [145]. In addition to reporting on the electron impact induced mass spectra we concentrated on their gas phase ion chemistry—specifically, the unimolecular fragmentations obtained through mass analyzed ion kinetic energy spectrometry. Unlike metal containing and noble gas containing endohedral fullerenes studied earlier, the ions N @ C_{60}^{+} and N @ C_{70}^{+} do not lose C_2 groups unimolecularly but lose the nitrogen atom instead. This indicates that the activation energy for the nitrogen atom loss

$$N@C_{60}^{+} \rightarrow C_{60}^{+} + N \qquad (7)$$
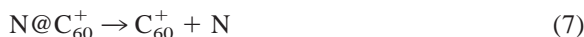
is lower than for the C_2 elimination from the cage

$$N@C_{60}^{+} \xrightarrow{\text{x}} N@C_{58}^{+} + C_2 \qquad (8)$$
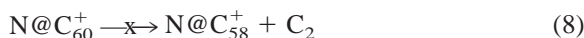
This was verified through the analysis of KERD measurements. The results were discussed in light of the thermal instability of nitrogen atom endohedral compounds compared to noble gas containing analogues. An autocatalytic bond breakage mechanism has been proposed for the ionic species, by analogy to the neutral, that requires less energy than the considerable cage distortion needed for penetration by a helium atom [reaction (5)].

An experiment was done by accurately dividing a sample in half; one half was heated at 230 °C for 4 h whereas the other half was used as a control. Fig. 12 represents the corresponding mass spectra showing clearly the loss of N@C_{60} signal upon heating demonstrating that the nitrogen atom escapes the cage of the neutral fullerene. Fig. 13 represents a characteristic KERD for reaction (7) of the ion from which the
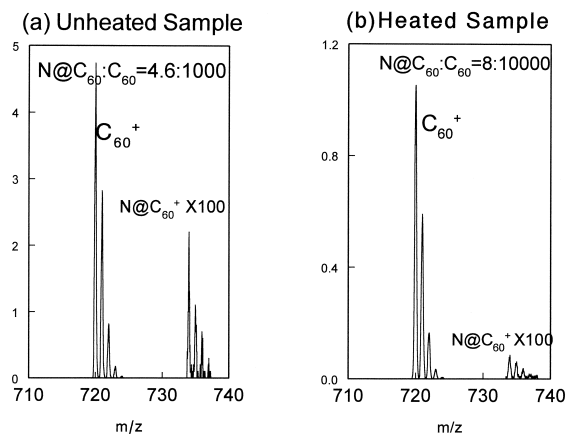

Fig. 12. Mass spectra of endohedral N@C_{60} containing samples. The sample was prepared by ion implantation [150]. One half was heated whereas the other was used as a control (see the text). Results given in [170].

activation energy limits for the nitrogen atom escape from the ionic fullerene were deduced by using the model-free approach [103,136,150]: $6.7 \lesssim \Delta E_{\text{vap}}(7) \lesssim 11.0$ eV. The lower limit corresponds to an Arrhenius pre-exponential A factor for reaction (7), $A = 10^{13}$ s^{-1}; the upper limit corresponds to $A = 3.5 \times 10^{17}$ s^{-1}, which is unrealistically high. Restricting the range of values of the pre-exponential A factor would restrict the range of activation energies deduced [150].

7. Some aspects of ion/molecule reactivity

D. K. Böhme has carried out a tour de force study of the bimolecular gas phase ion chemistry of singly and multiply charged fullerene ions with various neutral reagents at room temperature using the selected-ion flow tube technique. A brief review of the work has appeared recently [151]. Both the nature of the product channel and the rate of reaction were observed to be a function of the charge state of C_{60}^{z+} with C_{60}^{+} being the least reactive. Fullerene cations containing adjacent pentagons such as C_{58}^{z+} and C_{56}^{z+} demonstrate enhanced reactivity [152].

C_{60}^{2+} is much more reactive than C_{60}^{+} in electron transfer reactions due its higher recombination
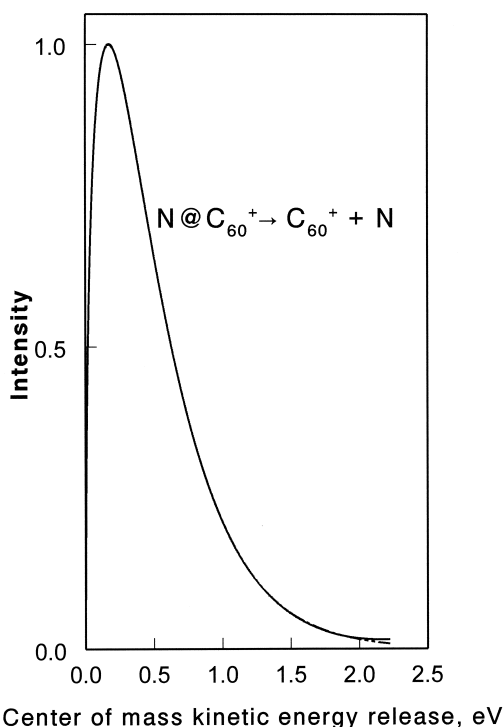
Fig. 13. Center of mass kinetic energy release distribution for the escape of the endohedral nitrogen atom from N @ C_{60}^+. Results given in [171].

energy. It is also more reactive in chemical bonding due to the stronger electrostatic interaction with neutral molecules [151]. Of special interest are its ionic polymerization reactions that proceed via a "ball-and-chain"' propagation. The sequential addition of allene to C_{60}^{2+} exhibits a striking periodicity, with the even numbered adducts reacting about 10 times faster than the odd numbered adducts, Fig. 14. The bond connectivity of these adducts was successfully probed [151] using multicollision induced dissociation.

8. Some final remarks

The discovery of carbon clusters and of fullerenes would not have taken place when it did without mass spectrometry. The mass spectrometric discovery led in turn to the synthesis and to the current enormous

successes in basic as well as applied research. Some of the recent efforts concern carbon nanotube technology, a topic that is predicted to have important industrial applications but is outside our present scope.

A point that is usually raised in cluster research is that clusters bridge the gap between isolated gas phase molecules and condensed matter. The properties we have discussed here like thermionic emission and blackbody radiation are well known for bulk matter. The question can be raised "how large is large?" Are the carbon clusters demonstrating delayed ionization really undergoing thermionic emission; is the continuous emission in the visible really blackbody radiation? These questions are still under debate. There are several other properties of C_{60} and other fullerenes that are characteristic of bulk matter. Hertel and co-workers [153] found one very important attribute through vacuum–ultraviolet (VUV) photoionization, namely the "giant" resonance at about 20 eV due to collective plasmon excitation. This had originally been predicted for C_{60} clusters by Bertsch et al. [154] and we have already alluded to this phenomenon in an earlier review [155]. We have since then observed giant plasmon excitations in the VUV photoionization of a series of polycyclic aromatic hydrocarbons [156] that are definitely smaller than C_{60}. So on the one hand, C_{60} is large enough to demonstrate bulk properties yet it is capable of wave behavior—the observation of de Broglie wave interference of C_{60} molecules by diffraction has been reported [157].

Carbon clusters, fullerenes and especially C_{60} have been a testing ground for statistical theories. The evaporative ensemble model (EEM) and FHBT [52,71,72,93,103,137,158–161] were particularly useful. Nevertheless, carbon clusters demonstrate some unique features, which set them apart from other clusters. For example, the EEM does not take into account cooling processes other than dissociative decay. As a result of radiative decay discussed above, the original dependence of the metastable fractions on reaction time deduced by EEM had to be revised [57–59]. The Gspann parameter, $\gamma = \ln A - \ln k(T_b)$ (where A is the Arrhenius pre-exponential factor and $k(T_b)$ is the most probable rate constant at the isoki-
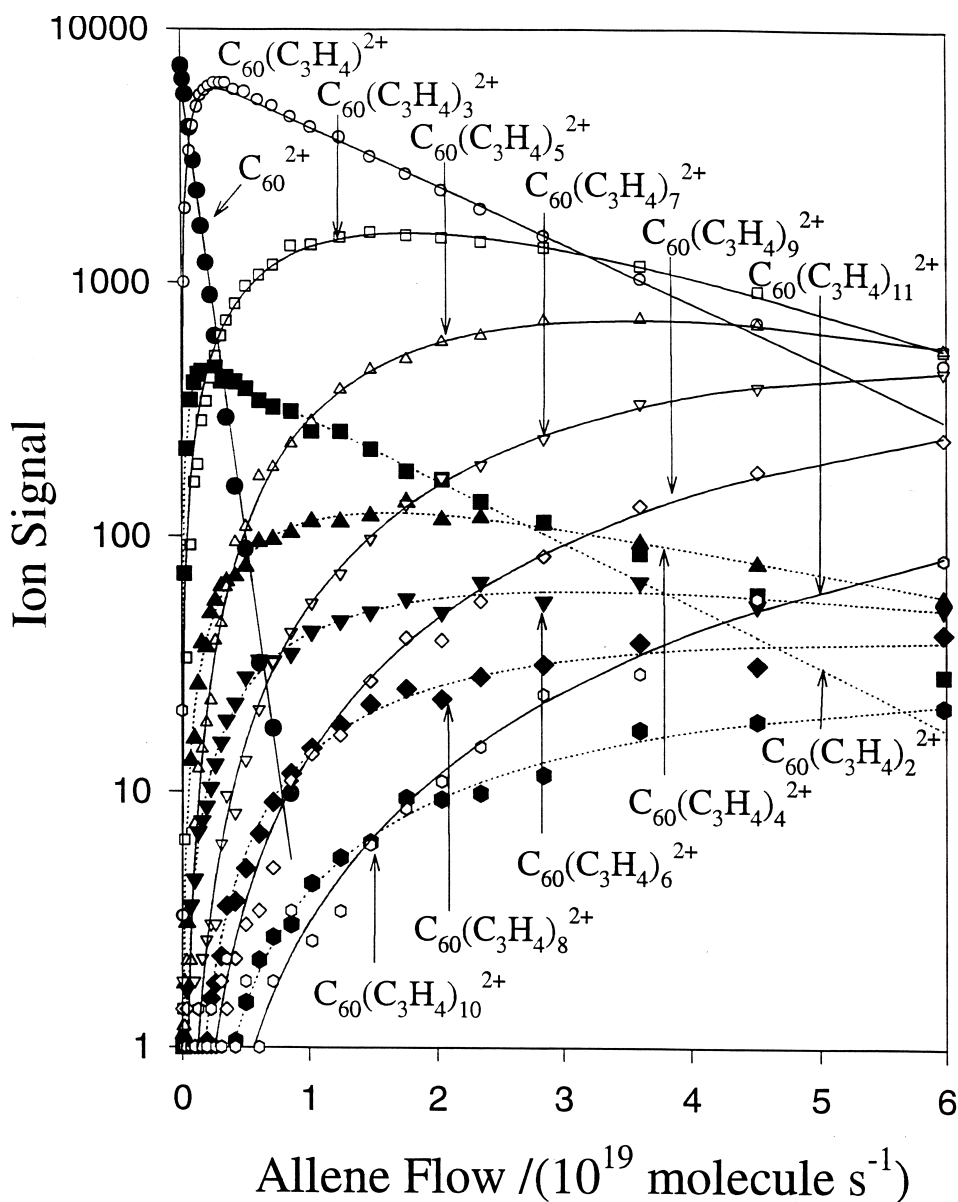
Fig. 14. Data for the sequential addition of allene to C_{60}^{2+} observed at a room temperature of 294 $\pm$ 2 K and a helium pressure of 0.35 $\pm$ 0.01 Torr; reproduced by permission from [151].

netic bath temperature T_b) was given a "best-value" [159,162] $\gamma = 23.5 \pm 1.5$. In other words, γ was considered to be a universal constant for all clusters of all sizes. However, it was eventually realized that C_{60} is unique and its Gspann parameter, γ may be as high as 37.6 [163], γ is time dependent [60] and is at least

equal to 33 on the microsecond time scale of most mass spectrometers [59,60,74].

So much has happened that was unforeseeable that predictions for the future seem dangerous. The ion chromatography method originally developed for the study of carbon clusters is now a most powerful

method in the study of conformations of gas phase biomolecules [164,165]. Other experimental methods such as photoionization by femtosecond lasers have just begun to give exciting new results for carbon clusters [7]. New experimental results concerning carbon clusters have forced the development of new theoretical approaches both for structure calculations and for the dynamics of evaporation and cooling. More advances along these lines are to be expected. It has become clear that experiments by themselves do not suffice. This has been most obvious in the elaborate analysis required for deducing the C_{58}–C_2 binding energy from appearance energy measurements [74,93].

Acknowledgements

References

[1] O. Hahn, F. Strassman, J. Mattauch, H. Ewald, Naturwissenschaften 36 (1942) 541; W. A. Chupka, M.G. Inghram, J. Chem. Phys. 22 (1954) 1472; J. Berkowitz, W.A. Chupka, ibid. 40 (1964) 2735.

[2] H.W. Kroto, J.R. Heath, S.C. O'Brian, R.F. Curl, R.E. Smalley, Nature 318 (1985) 162.

[3] E.A. Rohlfing, D.M. Cox, A. Kaldor, J. Chem. Phys. 81 (1984) 3322.

[4] H. Kroto, Science 242 (1988) 1139.

[5] P. Wurz, K.R. Lykke, Chem. Phys. 184 (1994) 335.

[6] P. Scheier, B. Dünser, R. Wörgötter, M. Lezius, R. Robl, T.D. Märk, Int. J. Mass Spectrom. Ion Processes 138 (1994) 77.

[7] M. Tchaplyguine, K. Hoffmann, O. Dühr, H. Hohmann, G. Korn, H. Rottke, M. Wittmann, I.V. Hertel, E.E.B. Campbell, J. Chem. Phys. 112 (2000) 2781.

[8] R.E. Smalley, Acc. Chem. Res. 25 (1992) 98.

[9] W. Krätschmer, L.D. Lamb, K. Fostiropoulos, D.R. Huffman, Nature 347 (1990) 354.

[10] S.W. McElvany, W.R. Creasy, A. O'Keefe, J. Chem. Phys. 85 (1986) 632.

[11] A. Van Orden, R.J. Saykally, Chem. Rev. 98 (1998) 2313.

[12] J.P. Maier, J. Phys. Chem. A 102 (1998) 3462.

[13] J.M.L. Martin, J. El-Yazal, J.P. Francois, Chem. Phys. Lett. 242 (1995) 570.

[14] K. Raghavachari, R.A. Whiteside, J.A. Pople, J. Chem. Phys. 85 (1986) 6623; J.M.L. Martin, P.R. Taylor, J. Phys. Chem. 100 (1996) 6047.

[15] S.W. McElvany, B.I. Dunlap, A. O'Keefe, J. Chem. Phys. 86 (1987) 715; D.C. Parent, S.W. McElvany, J. Am. Chem. Soc. 111 (1988) 2393.

[16] G. von Helden, M.-T. Hsu, P.R. Kemper, M.T. Bowers, J. Chem. Phys. 95 (1991) 3835.

[17] M.T. Bowers, P.R. Kemper, G. von Helden, P.A.M. van Koppen, Science 260 (1993) 1446.

[18] G. von Helden, N.G. Gotts, M.T. Bowers, Chem. Phys. Lett. 212 (1993) 241.

[19] (a) G. von Helden, M.T. Hsu, N. Gotts,, M.T. Bowers, J. Phys. Chem. 97 (1993) 8182; (b) G. von Helden, N.G. Gotts, M.T. Bowers, Nature 363 (1993) 60; (c) J. Am. Chem. Soc. 115 (1993) 4363.

[20] G. von Helden, N.G. Gotts, W.E. Palke, M.T. Bowers, Int. J. Mass Spectrom. Ion Processes 138 (1994) 33.

[21] G. von Helden, P.R. Kemper, N.G. Gotts, M.T. Bowers, Science 259 (1993) 1300.

[22] N.G. Gotts, G. von Helden, M.T. Bowers, Int. J. Mass Spectrom. Ion Processes 149/150 (1995) 217.

[23] J. Hunter, J. Fye, M.F. Jarrold, J. Phys. Chem. 97 (1993) 3460.

[24] J.M. Hunter, J.L. Fye, M.F. Jarrold, J. Chem. Phys. 99 (1993) 1785.

[25] J.M. Hunter, J.L. Fye, E.J. Roskamp, M.F. Jarrold, J. Phys. Chem. 98 (1994) 1810.

[26] K.B. Shelimov, J.M. Hunter, M.F. Jarrold, Int. J. Mass Spectrom. Ion Processes 138 (1994) 17.

[27] J. Hunter, J. Fye, M.F. Jarrold, Science 260 (1993) 784.

[28] J.D. Presilla-Marquez, J.A. Sheehy, J.D. Mills, P.G. Carrick, C.W. Larson, Chem. Phys. Lett. 274 (1997) 439.

[29] R. Hoffmann, Tetrahedron 22 (1966) 521.

[30] S. Yang, K.J. Taylor, M.J. Craycraft, J. Conceicao, C.L. Pettiette, O. Cheshnovsky, R.E. Smalley, Chem. Phys. Lett. 144 (1988) 431.

[31] C. Liang, H.F. Schaefer III, J. Chem. Phys. 93 (1990) 8844.

[32] C. Lifshitz, P. Sandler, H.-Fr. Grützmacher, J. Sun, T. Weiske, H. Schwarz, J. Phys. Chem. 97 (1993) 6592.

[33] J. Sun, H.-Fr. Grützmacher, C. Lifshitz, J. Am. Chem. Soc. 115 (1993) 8382.

[34] J. Sun, H.-Fr. Grützmacher, C. Lifshitz, J. Phys. Chem. 98 (1994) 4536.

[35] J. Sun, H.-Fr. Grützmacher, C. Lifshitz, Int. J. Mass Spectrom. Ion Processes 138 (1994) 49.

[36] B. Pozniak, R.C. Dunbar, J. Am. Chem. Soc. 118 (1994) 4113.

[37] B. Pozniak, R.C. Dunbar, J. Am. Chem. Soc. 119 (1997) 7343.

[38] C. Lifshitz, T. Peres, S. Kababia, I. Agranat, Int. J. Mass Spectrom. Ion Processes 82 (1988) 193.

[39] C. Lifshitz, T. Peres, I. Agranat, Int. J. Mass Spectrom. Ion Processes 93 (1989) 149.

[40] G. von Helden, E. Porter, N.G. Gotts, M.T. Bowers, J. Phys. Chem. 99 (1995) 7707.

[41] G. von Helden, M.T. Hsu, N.G. Gotts, P.R. Kemper, M.T. Bowers, Chem. Phys. Lett. 204 (1993) 15.

[42] P.R. Taylor, E. Bylaska, J.H. Weare, R. Kawai, Chem. Phys. Lett. 235 (1995) 558; J.M.L. Martin, J. El-Yazal, J.P. Francois, ibid. 248 (1996) 345; J.C. Grossman, L. Mitas, K. Raghavachari, Phys. Rev. Lett. 75 (1995) 3870.

[43] J.M.L. Martin, J. El-Yazal,, J.P. Francois, Chem. Phys. Lett. 255 (1996) 7.

[44] E.E.B. Campbell, R.D. Levine, Annu. Rev. Phys. Chem. 51 (2000) 65.

[45] R. Mitzner, E.E.B. Campbell, J. Chem. Phys. 103 (1995) 2445.

[46] E. Kolodney, A. Budrevich, B. Tsipinyuk, Phys. Rev. Lett. 74 (1995) 510.

[47] J.U. Andersen, C. Brink, P. Hvelplund, M.O. Larsson, B. Bech Nielsen, H. Shen, Phys. Rev. Lett. 77 (1996) 3991.

[48] C. Brink, L.H. Andersen, P. Hvelplund, D. Mathur, J.D. Voldstad, Chem. Phys. Lett. 233 (1995) 52.

[49] X.-B. Wang, C.-F. Ding, L.-S. Wang, J. Chem. Phys. 110 (1999) 8217.

[50] J. Lemaire, M. Heninger, R. Marx, G. Mauclaire, Int. J. Mass Spectrom. 189 (1999) 93.

[51] W.A. Chupka, C.E. Klots, Int. J. Mass Spectrom. Ion Processes 167/168 (1997) 595.

[52] C.E. Klots, Int. Rev. Phys. Chem. 15 (1996) 205.

[53] C. Lifshitz, I. Gotkis, P. Sandler, J. Laskin, Chem. Phys. Lett. 200 (1992) 406.

[54] J. Laskin, J.M. Behm, K.R. Lykke, C. Lifshitz, Chem. Phys. Lett. 252 (1996) 277.

[55] R. Wörgötter, B. Dünser, P. Scheier, T. D. Märk, J. Chem. Phys. 101 (1994) 8674.

[56] S. Matt, D. Muigg, A. Ding, C. Lifshitz, P. Scheier, T.D. Märk, J. Phys. Chem. 100 (1996) 8692.

[57] K. Hansen, E.E.B. Campbell, J. Chem. Phys. 104 (1996) 5012.

[58] J. Laskin, C. Lifshitz, Chem. Phys. Lett. 277 (1997) 564.

[59] J. Laskin, B. Hadas, T. D. Märk, C. Lifshitz, Int. J. Mass Spectrom. 177 (1998) L9.

[60] S. Matt, R. Parajuli, A. Stamatovic, P. Scheier, T.D. Märk, J. Laskin, C. Lifshitz, Eur. Mass Spectrom. 5 (1999) 477.

[61] S. Maruyama, M.Y. Lee, R.E. Haufler, Y. Chai, R.E. Smalley, Z. Phys. D 19 (1991) 409.

[62] E.E.B. Campbell, G. Ulmer, I.V. Hertel, Phys. Rev. Lett. 67 (1991) 1986.

[63] P. Wurz, K.R. Lykke, J. Chem. Phys. 95 (1991) 7008.

[64] E.E.B. Campbell, K. Hansen, K. Hoffmann, G. Korn, M. Tchaplyguine, M. Wittmann, I.V. Hertel, Phys. Rev. Lett. 84 (2000) 2128.

[65] P. Wurz, K.R. Lykke, J. Phys. Chem. 96 (1992) 10129.

[66] M. Hippler, M. Quack, R. Schwarz, G. Seyfang, S. Matt, T. Märk, Chem. Phys. Lett. 278 (1997) 111.

[67] L.S. Wang, J. Conceicao, C.M. Jin, R.E. Smalley, Chem. Phys. Lett. 182 (1991) 5.

[68] K. Hansen, J.U. Andersen. H. Cederquist, C. Gottrup, P. Hvelplund, M.O. Larsson, V.V. Petrunin, H.T. Schmidt, Eur. Phys. J. D 9 (1999) 351.

[69] E.E.B. Campbell, R.D. Levine, Comments Mod. Phys. 1 (1999) 155.

[70] D. Ding, R.N. Compton, R.E. Haufler, C.E. Klots, J. Phys. Chem. 97 (1993) 2500; Y. Zhang, M. Stuke, Phys. Rev. Lett. 70 (1993) 3231.

[71] C.E. Klots, Chem. Phys. Lett. 186 (1991) 73.

[72] P. Sandler, C. Lifshitz, C.E. Klots, Chem. Phys. Lett. 200 (1992) 445.

[73] Z. Wan, J.F. Christian, Y. Basir, S.L. Anderson, J. Chem. Phys. 99 (1993) 5858.

[74] C. Lifshitz, Int. J. Mass Spectrom. 198 (2000) 1.

[75] H. Steger, J. de Vries, B. Kamke, W. Kamke, T. Drewello, Chem. Phys. Lett. 194 (1992) 452.

[76] D.K. Böhme, Int. Rev. Phys. Chem. 13 (1994) 163.

[77] K.W. Kennedy, O. Echt, J. Phys. Chem. 97 (1993) 7088.

[78] R. Deng, O. Echt, J. Phys. Chem. A 102 (1998) 2533.

[79] K. Hansen, O. Echt, Phys. Rev. Lett. 78 (1997) 2337.

[80] C. Lifshitz, Current Topics in Ion Chemistry, Physics: Clusters, T. Baer, C.Y. Ng, I. Powis (Eds.), Wiley, New York, 1993.

[81] P.P. Radi, T.L. Bunn, P.R. Kemper, M.E. Molchan, M.T. Bowers, J. Chem. Phys. 88 (1988) 2809.

[82] P.P. Radi, M.E. Rincon, M.-T. Hsu, J. Brodbelt-Lustig, P. Kemper, M.T. Bowers, J. Phys. Chem. 93 (1989) 6187.

[83] P.P. Radi, M.T. Hsu, J. Brodbelt-Lustig, M. Rincon, M.T. Bowers, J. Chem. Phys. 92 (1990) 4817.

[84] P.P. Radi, M.-T. Hsu, M.E. Rincon, P.R. Kemper, M.T. Bowers, Chem. Phys. Lett. 174 (1990) 223.

[85] M.T. Bowers, P.P. Radi, M.-T. Hsu, J. Chem. Phys. 94 (1991) 6934.

[86] D.R. Luffer, K.H. Schram, Rapid Commun. Mass Spectrom. 4 (1990) 552.

[87] K.A. Caldwell, D.E. Giblin, M.L. Gross, J. Am. Chem. Soc. 114 (1992) 3743.

[88] S.C. O'Brien, J.R. Heath, R.F. Curl, R.E. Smalley, J. Chem. Phys. 88 (1988) 220.

[89] M. Foltin, O. Echt, P. Scheier, B. Dünser, R. Wörgötter, D. Muigg, S. Matt, T. D. Märk, J. Chem. Phys. 107 (1997) 6246.

[90] M.J. Polce, S. Beranová, M.J. Nold, C. Wesdemiotis, J. Mass Spectrom. 31 (1996) 1073.

[91] M. Foltin, M. Lezius, P. Scheier, T.D. Märk, J. Chem. Phys. 98 (1993) 9624.

[92] T. Drewello, W. Krätschmer, M. Fieber-Erdmann, A. Ding, Int. J. Mass Spectrom. Ion Processes 124 (1993) R1.

[93] R. Wörgöotter, B. Dünser, P. Scheier, T. D. Märk, M. Foltin, C.E. Klots, J. Laskin, C. Lifshitz, J. Chem. Phys. 104 (1996) 1225.

[94] A.D. Boese, G.E. Scuseria, Chem. Phys. Lett. 294 (1998) 233.

[95] J. Laskin, T. Peres, A. Khong, H.A. Jiménez-Vázquez, R.J. Cross, M. Saunders, D.S. Bethune, M.S. de Vries, C. Lifshitz, Int. J. Mass Spectrom. Ion Processes 185/186/187 (1999) 61.

[96] S. Matt, M. Sonderegger, R. David, O. Echt, P. Scheier, J. Laskin, C. Lifshitz, T.D. Märk, Int. J. Mass Spectrom. Ion Processes 185/186/187 (1999) 813.

[97] S. Matt, O. Echt, M. Sonderegger, R. David, P. Scheier, J. Laskin, C. Lifshitz, T.D. Märk, Chem. Phys. Lett. 303 (1999) 379.

[98] R.L. Murry, D.L. Strout, G.K. Odom, G.E. Scuseria, Nature (London) 366 (1993) 665.

[99] W.C. Eckhoff, G.E. Scuseria, Chem. Phys. Lett. 216 (1993) 399.

[100] C. Xu, G.E. Scuseria, Phys. Rev. Lett. 72 (1994) 669.

[101] M.B. Sowa, P.A. Hintz, S.L. Anderson, J. Chem. Phys. 95 (1991) 4719.

[102] M.B. Sowa-Resat, P.A. Hintz, S.L. Anderson, J. Phys. Chem. 99 (1995) 10736.

[103] C.E. Klots, Z. Phys. D 21 (1991) 335.

[104] J. Laskin, C. Lifshitz, Int. J. Mass Spectrom. Ion Processes 138 (1994) 95.

[105] P.E. Barran, S. Firth, A.J. Stace, H.W. Kroto, K. Hansen, E.E.B. Campbell, Int. J. Mass Spectrom. Ion Processes 167/168 (1997) 127.

[106] S. Matt, O. Echt, R. Wörgötter, P. Scheier, C.E. Klots, T. D. Märk, Int. J. Mass Spectrom. Ion Processes 167/168 (1997) 753.

[107] B.L. Zhang, C.H. Xu, C.Z. Wang, C.T. Chan, K.M. Ho, Phys. Rev. B 46 (1992) 7333.

[108] J.F. Christian, Z. Wan, S.L. Anderson, J. Chem. Phys. 99 (1993) 3468.

[109] P. Scheier, T.D. Märk, Phys. Rev. Lett. 73 (1994) 54.

[110] P. Scheier, B. Dünser, T. D. Märk, J. Phys. Chem. 99 (1995) 15428.

[111] P. Scheier, B. Dünser, T. D. Märk, Phys. Rev. Lett. 74 (1995) 3368.

[112] B. Dünser, O. Echt, P. Scheier, T. D. Märk, Phys. Rev. Lett. 79 (1997) 3861.

[113] P.W. Gill, L.J. Radom, J. Am. Chem. Soc. 110 (1988) 5311.

[114] R.D. Beck, P. St. John, M.M. Alvarez, F. Diederich, R.L. Whetten, J. Phys. Chem. 95 (1991) 8402.

[115] C. Yeretzian, R.D. Beck, R.L. Whetten, Int. J. Mass Spectrom. Ion Processes 135 (1994) 79.

[116] C. Yeretzian, R.L. Whetten, Z. Phys. D 24 (1992) 199.

[117] C. Yeretzian, K. Hansen, F. Diederich, R.L. Whetten, Nature 44 (1992) 359.

[118] P. Weis, J. Rockenberger, R.D. Beck, M.M. Kappes, J. Chem. Phys. 104 (1996) 3629.

[119] R.D. Beck, J. Rockenberger, P. Weis, M.M. Kappes, J. Chem. Phys. 104 (1996) 3638.

[120] H. Hohmann, C. Callegari, S. Furrer, D. Grosenick, E.E.B. Campbell, I.V. Hertel, Phys. Rev. Lett. 73 (1994) 1919.

[121] P. Hvelplund, L.H. Andersen, H.K. Haugen, J. Linhard, D.C. Lorents, R. Malhotra, R. Ruoff, Phys. Rev. Lett. 69 (1992) 1915.

[122] R. Ehlich, M. Westenburg, E.E.B. Campbell, J. Chem. Phys. 104 (1996) 1900.

[123] T. Fiegele, O. Echt, F. Biasioli, C. Mair, T.D. Märk, Chem. Phys. Lett. 316 (2000) 387.

[124] S.G. Kim, D. Tomanek, Phys. Rev. Lett. 72 (1994) 2418; S. Serra, S. Sanguinetti, L. Colombo, J. Chem. Phys. 102 (1995) 2151.

[125] E.E.B. Campbell, T. Raz, R.D. Levine, Chem. Phys. Lett. 253 (1996) 261.

[126] J.R. Heath, S.C. O'Brien, Q. Zhang, Y. Liu, R.F. Curl, H.W. Kroto, F.K. Tittel, R.E. Smalley, J. Am. Chem. Soc. 107 (1985) 7779.

[127] (a)Y. Chai, T. Guo, C. Jin, R.E. Haufler, L.P.F. Chibante, J. Fure, L. Wang, J.M. Alford, R.E. Smalley, J. Phys. Chem. 95(1991) 7564; (b). R.D. Johnson, M.S. de Vries, J.R. Salem, D.S. Bethune, C.S. Yanoni, Nature, 355 (1992) 239.

[128] T. Weiske, D.K. Böhme, J. Hrusák, W. Krätchmer, H. Schwarz, Angew. Chem. Int. Ed. 30 (1991) 884.

[129] T. Weiske, J. Hrusák, D.K. Böhme, H. Schwarz, Helv. Chim. Acta 75 (1992) 79.

[130] M. Saunders, H.A. Jiménez-Vázquez, R.J. Cross, R.J. Poreda, Science 259 (1993) 1428.

[131] M. Saunders, H.A. Jiménez-Vázquez, R.J. Cross, S. Mroczkowski, M.L. Gross, D.E. Giblin, R.J. Poreda, J. Am. Chem. Soc. 116 (1994) 2193.

[132] L. Becker, R.J. Poreda, T.E. Bunch, Proc. Natl. Acad. Sci. USA 97 (2000) 2979.

[133] F.D. Weiss, J.L. Elkind, S.C. O'Brien, R.F. Curl, R.E. Smalley, J. Am. Chem. Soc. 110 (1988) 4464.

[134] J. Laskin, H.A. Jiménez-Vázquez, R. Shimshi, M. Saunders, M.S. de Vries, C. Lifshitz, Chem. Phys. Lett. 242 (1995) 249.

[135] J. Laskin, T. Peres, A. Khong, H.A. Jiménez-Vázquez, R.J. Cross, M. Saunders, D.S. Bethune, M.S. de Vries, C. Lifshitz, Int. J. Mass Spectrom. 185/186/187 (1999) 61.

[136] P. Sandler, T. Peres, G. Weissman, C. Lifshitz, Ber. Bunsenges. Phys. Chem. 96 (1992) 1195.

[137] C.E. Klots, J. Chem. Phys. 98 (1993) 1110; 100 (1994) 1035.

[138] J. Laskin, T. Peres, C. Lifshitz, M. Saunders, R.J. Cross, A. Khong, Chem. Phys. Lett. 285 (1998) 7.

[139] A. Khong, H.A. Jiménez-Vázquez, M. Saunders, R.J. Cross, J. Laskin, T. Peres, C. Lifshitz, R. Strongin, A.B. Smith III, J. Am. Chem. Soc. 120 (1998) 6380.

[140] S. Patchkovskii, W. Thiel, J. Am. Chem. Soc. 118 (1996) 7164; Helv. Chim. Acta 80 (1997) 495.

[141] T. Weiske, H. Schwarz, Angew. Chem. Int. Ed. Engl. 31 (1992) 605.

[142] R. Tellgmann, N. Krawez, S.-H. Lin, I.V. Hertel, E.E.B. Campbell, Nature 382 (1996) 407.

[143] R. Shimshi, R.J. Cross, M. Saunders, J. Am. Chem. Soc. 119 (1997) 1163.

[144] R.J. Cross, M. Saunders, H. Prinzbach, Org. Lett. 1 (1999) 1479.

[145] T. Almeida Murphy, Th. Pawlik, A. Weidinger, M. Höhne, R. Alcala, J.-M. Spaeth, Phys. Rev. Lett. 77 (1996) 1075.

[146] A. Weidinger, M. Waiblinger, B. Pietzak, T. A. Murphy, Appl. Phys. A 66 (1998) 1.

[147] B. Pietzak, M. Waiblinger, T. A. Murphy, A. Weidinger, M. Höhne, E. Dietel, A. Hirsch, Chem. Phys. Lett. 279 (1997) 259.

[148] C. Knapp, K.-P. Dinse, B. Pietzak, M. Waiblinger, A. Weidinger, Chem. Phys. Lett. 272 (1997) 433.

[149] E. Dietel, A. Hirsch, B. Pietzak, M. Waiblinger, K. Lips, A. Weidinger, A. Gruss, K.-P. Dinse, J. Am. Chem. Soc. 121 (1999) 2432.

[150] B. Cao, T. Peres, R. J. Cross, M. Saunders, C. Lifshitz, J. Phys. Chem. A, in press, ASAP.

[151] D.K. Böhme, Can. J. Chem. 77 (1999) 1453.

[152] S. Petrie, D.K. Böhme, Nature (London) 365 (1993) 426.

[153] I.V. Hertel, H. Steger, J. de Vries, B. Weisser, C. Menzel, B. Kamke, W. Kamke, Phys. Rev. Lett. 68 (1992) 784.

[154] G.F. Bertsch, A. Bulgac, D. Tomanek, Y. Wang, Phys. Rev. Lett. 67 (1991) 2690.

[155] C. Lifshitz, Mass Spectrom. Rev. 12 (1993) 261.

[156] Y. Ling, C. Lifshitz, Chem. Phys. Lett. 257 (1996) 587.

[157] M. Arndt, O. Nairz, J. Vos-Andreae, C. Keller, G. van der Zouw, A. Zeilinger, Nature (London) 401 (1999) 680.

[158] C.E. Klots, in Current Topics in Ion Chemistry, Physics: Clusters, T. Baer. C.Y. Ng, I. Powis (Eds.), Wiley, New York, 1994.

[159] C.E. Klots, Z. Phys. D 20 (1991) 105.

[160] C.E. Klots, Z. Phys. D 5 (1987) 83.

[161] C.E. Klots, J. Phys. Chem. 92 (1988) 5864.

[162] C.E. Klots, Int. J. Mass Spectrom. Ion Processes 100 (1990) 457.

[163] V. Foltin, M. Foltin, S. Matt, P. Scheier, K. Becker, H. Deutsch, T.D. Märk, Chem. Phys. Lett. 289 (1998) 181.

[164] T. Wyttenbach, G. von Helden, M.T. Bowers, J. Am. Chem. Soc. 118 (1996) 8355.

[165] S.J. Valentine, D.E. Clemmer, J. Am. Chem. Soc. 119 (1997) 3558.

[166] J. Laskin, Ph.D. thesis, The Hebrew University of Jerusalem, 1998.

[167] B. Cao, W. Cui, T. Peres, R. Cohen, M. de Vries, C. Lifshitz, unpublished results (1999).

[168] A. Khong, T. Peres, R.J. Cross, M. Saunders, C. Lifshitz, unpublished results (1999).

[169] T. Peres, E. Campbell, C. Lifshitz, unpublished results (1999).

[170] T. Peres, B. Cao, R.J. Cross, M. Saunders, C. Lifshitz, unpublished results (2000).

[171] T. Peres, B. Cao, R.J. Cross, M. Saunders, C. Lifshitz, unpublished results (1999).